# Coastal Systems Station, Dahlgren Division
# Naval Surface Warfare Center
Panama City, Florida 32407-7001

## AD-A257 619

# EFFECTS OF QUADRATIC NONLINEARITIES

# ON THE RESPONSE OF INDIVIDUAL MODES

# OF TOWED CABLE SYSTEMS

# UNDER TOW POINT EXCITATION

J. W. KAMMAN

**DTIC**
**S** **ELECTE**
**NOV25 1992**
**E** **D**

**DESTRUCTION NOTICE**

For unclassified limited documents, destroy by any method that will prevent disclosure of contents or reconstruction of the document.

**92-30234**

## CSS TM 628-92
# Coastal Systems Station, Dahlgren Division
# Naval Surface Warfare Center
PANAMA CITY, FLORIDA 32407-7001

CAPT D. C. STEERE, USN
Commanding Officer

MR. TED C. BUCKLEY
Executive Director

## ADMINISTRATIVE INFORMATION

Released by
D. P. SKINNER, Head
Coastal Research and Technology Department

Under authority of
T. C. BUCKLEY
Executive Director

# REPORT DOCUMENTATION PAGE

Public reporting burden for this collection of information is estimated to average 1 hour per response, including the time for reviewing instructions, searching existing data sources, gathering and maintaining the data needed, and completing and reviewing the collection of information. Send comments regarding this burden estimate or any other aspect of this collection of information, including suggestions for reducing this burden, to Washington Headquarters Services, Directorate for Information Operations and Reports, 1215 Jefferson Davis Highway, Suite 1204, Arlington, VA 22202-4302, and to the Office and Management and Budget, Paperwork Reduction Project (0704-0188), Washington, DC 20503.

| 1. AGENCY USE ONLY (Leave blank) | 2. REPORT DATE | 3. REPORT TYPE AND DATES COVERED |
|---|---|---|
| | November 1992 | |

**4. TITLE AND SUBTITLE**
Effects of Quadratic Nonlinearities on the Response of Individual Modes of Towed Cable Systems Under Tow Point Excitation

**5. FUNDING NUMBERS**

**6. AUTHOR(S)**
J. W. Kamman

**7. PERFORMING ORGANIZATION NAME(S) AND ADDRESS(ES)**

Coastal Systems Station Dahlgren Division
Naval Surface Warfare Center
Code 1210
6703 West Highway 98
Panama City, FL 32407-7001

**8. PERFORMING ORGANIZATION REPORT NUMBER**

CSS TM 628-92

**9. SPONSORING/MONITORING AGENCY NAME(S) AND ADDRESS(ES)**

Office of Naval Technology
800 North Quincy Street
Arlington, VA 22217-5000

**10. SPONSORING/MONITORING AGENCY REPORT NUMBER**

**11. SUPPLEMENTARY NOTES**

**12a. DISTRIBUTION/AVAILABILITY STATEMENT**
Approved for public release; distribution is unlimited.

**12b. DISTRIBUTION CODE**

**13. ABSTRACT (Maximum 200 words)**

Underwater towed systems are very important to many marine applications. To date, many methods of analysis have been developed to simulate the dynamic behavior of these systems. The models that result from these methods can be separated into two categories - linear and nonlinear models. Linear models provide insight into the underlying system dynamics but only near steady-state configurations. Fully nonlinear models can simulate the dynamics of these systems undergoing arbitrary motions but produce equations of motion (EOM) that are very complex. This paper presents a methodology for understanding the first-order effects of the quadratic nonlinearities present in the EOM of nonlinear models. Specifically, the EOM produced by DYNTOCABS (a computer program in use at the Coastal Systems Station) are numerically reduced to form a set of equations that govern the modal response of the system to tow point excitation. The method of multiple scales is then used to analyze the effects of these nonlinearities on the response of individual modes. Results are given for two modes of a simple towed system. They suggest that out-of-plane modes respond linearly to out-of-plane excitations, while in-plane modes can respond in a relatively strong nonlinear fashion to in-plane excitations.

**14. SUBJECT TERMS**
towed systems, cable dynamics, finite segment model, nonlinear perturbation analysis, model response

**15. NUMBER OF PAGES**
30

**16. PRICE CODE**

| 17. SECURITY CLASSIFICATION OF REPORT | 18. SECURITY CLASSIFICATION OF THIS PAGE | 19. SECURITY CLASSIFICATION OF ABSTRACT | 20. LIMITATION OF ABSTRACT |
|---|---|---|---|
| UNCLASSIFIED | UNCLASSIFIED | UNCLASSIFIED | |

# CONTENTS

| Accesion For | | |
|---|---|---|
| NTIS CRA&I | | ☒ |
| DTIC TAB | | ☐ |
| Unannounced | | ☐ |
| Justification | | |
| By _____ | | |
| Distribution / | | |
| Availability Codes | | |
| Dist | Avail and / or Special | |
| A-1 | | |

# ILLUSTRATIONS

# INTRODUCTION

Understanding of the dynamic response of underwater towed systems has been of interest for many years. In response to this need, many computer programs have been developed over the past 30 years to model this response; these computer programs are based on a number of methods including the continuum, finite element, finite segment, and lumped parameter approaches. References 1 through 11 describe the underlying methodologies for some of the codes in existence today. Although the calibration and validation of these codes is not always straight forward, it is generally believed that they capture the basic dynamics of these systems.

Many of these codes generate a set of nonlinear equations of motion that are numerically integrated to determine the two or three dimensional motion of the system over a specified interval of time. Because these codes function in the time-domain, they may be used to perform "numerical experiments" to gain insight into the fundamental dynamics of these systems. However, this is at best a trial-and-error process because the equations of motion generated and solved by the codes are quite complex, and in themselves, provide few useful hints about the overall system behavior.

Alternatively, some of the codes[1][10] break down dynamic response into a fewer number of response modes of the system. In particular, Reference 1 discusses the classical normal mode response of the system based on a numerical linearization of the nonlinear equations of motion about a stationary steady-state equilibrium. As Reference 12 suggests, this approach offers significant insight into the dynamical response of the system and into how this response is affected by various system parameters. Also, by comparing the linear and nonlinear responses by time domain simulation, nonlinear effects can be identified and evaluated. By this latter procedure, References 1 and 5 recognized the nonsymmetric response of a towed sphere under tow point excitation to be a result of system nonlinearities.

This paper presents an overview of a procedure that combines the strictly numerical finite segment approach presented in References 5 and 9 with the nonlinear analytical perturbation method of multiple scales[13][14]. This approach involves a two-step process. First, the fully-coupled three-dimensional nonlinear equations of motion for a finite segment model of a towed system are decomposed about a stationary steady-state equilibrium position into a set of equations in modal (or normal) variables; only quadratic nonlinearities are maintained in this process. These complex-valued equations are completely uncoupled in their linear terms, but in general, they remain coupled through the nonlinear terms. Inspection of these equations tells which modes are coupled at this level of approximation. Next, the method of multiple scales may be applied to these equations to determine the effects of quadratic nonlinearities on the response of single modes or on the interactions between modes of the system under tow point excitation. This report outlines the application of multiple scales to the response of a single mode only; application to mode coupling will be presented in a future report.

This approach combines the benefits of both numerical and analytical methods. Equations of motion about general steady-state configurations can be generated for complex systems, and after modal decomposition, analytical procedures can be applied to gain insight into the modal response of the system about those configurations.

The balance of this report is divided into five sections. The first discusses the full nonlinear equations of motion of a towed system and how they can be reduced to describe motions about stationary steady-state configurations; terms up through quadratic nonlinearities are maintained in the process. The second describes the modal decomposition and solution of the linearized equations. The third discusses a set of reduced nonlinear equations for the modal variables in which the modes of the system are coupled through the quadratic nonlinearities. The fourth section presents the methodology for the application of the method of multiple scales to determine the effects of the nonlinearities on the response of single underdamped modes of the system; it also includes results computed for two modes of a towed sphere with excitations both in and normal to the towed end of the cable. The final section contains a short summary.

## EQUATIONS OF MOTION

### NONLINEAR EQUATIONS

In this paper, a towed cable system is assumed to be a single or multiple branched cable system with towed bodies. The system is assumed to be towed from a single point. The cable branches form an open-tree system having no closed kinematic chains. Each length of cable may have different physical properties, and the towed bodies may be simple spheres or more sophisticated underwater vehicles. The motion of the system tow point is arbitrary. Figure 1 depicts a single branched system with a towed body.

These systems may be modeled by segmenting the cable into a series of discrete rigid links connected end-to-end using frictionless spherical joints. In general, the equations of motion of these so-called finite-segment models may be written in the form

$$\dot{x}_i = f_i(x_j) = x_{N+i} \quad (i = 1, \dots, N; j = 1, \dots, 2N) \tag{1}$$

$$\dot{x}_i = f_i(x_j, u_k) \quad (i = N+1, \dots, 2N; j = 1, \dots, 2N; k = 1, \dots, M) \tag{2}$$

where, for example, the $x_i(i = 1, \dots, N)$ may represent the orientation angles of the cable links and the towed vehicles relative to some reference frame, the $x_i(i = N+1, \dots, 2N)$ represent the first derivatives of these angles, and the $u_k(k = 1, \dots, M)$ represent external inputs such as motions of the system's tow point and motions of the towed vehicles' control flaps. There are many different analytical approaches that can be used to provide the equations in this form; the methodology used in this work is outlined in Reference 5.

During steady forward or steady (circular) turning motion, and in the absence of external disturbances, a towed system exhibits stationary steady-state equilibrium positions. In these situations, $x_i(i = 1, \dots, N)$ the orientation angles of the links and towed vehicles relative to the mean ship frame remain constant. In this case, the right sides of equations (1) and (2) are zero, and the angles defining the equilibrium shape of the system may be found by solving the $N$ nonlinear algebraic equations

$$f_{N+i}(x_j^e; u_k^e) = 0 \quad (i,j = 1,...,N; k = 1,...,M) \tag{3}$$

where the $x_j^e$ and $u_k^e$ represent the equilibrium values of the orientation angles and the external inputs, respectively.

Numerically solving Equations (3) for the steady-state equilibrium orientation angles can be difficult unless guesses very near the equilibrium values are used to initialize the solution process. In practice, these equations can be replaced by a series of smaller sets of equations that can be solved sequentially, allowing for a much more rapid and effective determination of the equilibrium angles. For example, the equilibrium equations for each body (cable links and towed vehicles) in the system may be written and solved as separate sets of equations so long as the solution process begins with equations associated with bodies at the ends of the branches and then proceeds from body to body towards the system tow point. For partially submerged systems or systems undergoing circular motion, this procedure is complicated somewhat. In these cases, the procedure must be repeated until convergence for the overall system occurs; however, this iteration process has generally been found to converge very rapidly.

## REDUCED NONLINEAR EQUATIONS - QUADRATIC NONLINEARITIES ONLY

To describe motions of the system that result from small disturbances to the state variables $x_i (i = 1,...,2N)$ and to the external input variables $u_k (k = 1,...,M)$, the right sides of the nonlinear Equations of motion (1) and (2) can be expanded in a Taylor Series about the equilibrium configuration defined by the solution of Equations (3). To this end, introduce the variables $y_i$ to represent perturbations of the equilibrium values of the state variables, and introduce the variables $v_k$ to represent perturbations of the equilibrium values of the external input variables so that

$$x_i = x_i^e + y_i \quad (i = 1,...,2N) \tag{4}$$

$$u_k = u_k^e + v_k \quad (k = 1,...,M). \tag{5}$$

Substituting these expressions into the nonlinear equations of motion, expanding in a Taylor Series about the equilibrium configuration, and omitting terms of third and higher order in the perturbations $y_i$ and $v_k$ results in equations of the form

$$\dot{y}_i = \sum_j A_{ij} y_j + \sum_k B_{ik} v_k + \frac{1}{2} \sum_{j,m} C_{ijm} y_j y_m + \frac{1}{2} \sum_{k,l} D_{ikl} v_k v_l + \sum_{j,k} E_{ijk} y_j v_k \tag{6}$$

where

$$A_{ij} = \left. \frac{\partial f_i}{\partial x_j} \right|_e \qquad B_{ik} = \left. \frac{\partial f_i}{\partial u_k} \right|_e \tag{7}$$

$$C_{ijm} = \left. \frac{\partial^2 f_i}{\partial x_j \partial x_m} \right|_e \qquad D_{ikl} = \left. \frac{\partial^2 f_i}{\partial u_k \partial u_l} \right|_e \qquad E_{ijk} = \left. \frac{\partial^2 f_i}{\partial x_j \partial u_k} \right|_e . \tag{8}$$

The subscript $e$ on the partial derivatives indicates that they are evaluated at the equilibrium configuration. Because the first $N$ equations of motion (Equations (1)) are simply definitions of the state variables $x_i$ ($i = N + 1, ..., 2N$), many of the $A_{ij}$, $B_{ik}$, $C_{ijm}$, $D_{ikl}$, and $E_{ijk}$ take on the values of *zero* or *one* and may be determined by inspection. All the other values may be approximated using finite differences; in this work, second-order central differences are used. Also, note that due to the equality between mixed second partial derivatives, the $C$ and $D$ arrays possess some symmetry so that $C_{ijm} = C_{imj}$ ($j, m = 1, ..., 2N$) and $D_{ikl} = D_{ilk}$ ($k, l = 1, ..., M$).

In the case of very small excursions from the steady state equilibrium position, Equations (6) may be further reduced by omitting the quadratic nonlinearities to give the linear equations

$$\dot{y}_i = \sum_j A_{ij} y_j + \sum_k B_{ik} v_k. \qquad (9)$$

## MODAL DECOMPOSITION OF LINEAR EQUATIONS OF MOTION

### EIGENVALUES AND EIGENVECTORS

The natural frequencies and corresponding mode shapes of the towed system motions described by the linear Equations (9) are determined by calculating the $2N$ eigenvalues and eigenvectors of the matrix A whose elements are the $A_{ij}$ ($i, j = 1, ..., 2N$). Typically, some of the eigenvalues will be real, and the remaining will occur in complex conjugate pairs. Assuming that the eigenvalues all have negative real parts (indicating that the steady state equilibrium is linearly stable), the real eigenvalues represent overdamped modes, and the complex ones represent underdamped modes. It will be assumed in the balance of this report that the steady state equilibrium is linearly stable and that A has $2N$ distinct eigenvalues and hence, $2N$ linearly independent eigenvectors.

As discussed in Reference 15, the eigenvector associated with the eigenvalue $\lambda_i$ takes the form

$$\mathbf{p}_i = \left\{ \frac{\{p^{(i)}\}}{\lambda_i \{p^{(i)}\}} \right\} \qquad (10)$$

where $\mathbf{p}_i$ is a $2N \times 1$ vector that can be partitioned into two $N \times 1$ vectors; as indicated in Equation (10), the bottom half vector is simply the product of the eigenvalue and the top half vector. The eigenvector is real-valued for real eigenvalues and complex-valued for complex eigenvalues. Moreover, eigenvectors that correspond to a pair of complex conjugate eigenvalues are themselves complex conjugates of each other.

The top half of the eigenvector represents the shape of the towed system. If the eigenvector is real-valued, then all points along the cable move in-phase as the mode is excited. However, if the eigenvector is complex, then there is a phase shift between the motions at different locations along the cable. Although the phase angle does vary along the cable, the relative phase shift between any two points along the cable is maintained as the cable moves. For example, it is not uncommon

4

for motion near the system tow point to be 180 degrees out of phase with the cable near the towed body. This is illustrated in Figure 2 that shows the steady-state configuration and five snap-shots of an in-plane mode of a 100-foot cable towing a 500-pound spherical body at 5 knots. The displacements have been magnified for clarity.

Finally, **P**, the "eigencolumn" or "modal" matrix of **A** is defined to be the $2N \times 2N$ matrix whose columns are formed from the eigenvectors of **A**. When the eigenvalues are all distinct, the modal matrix can be used to diagonalize **A** as follows:

$$\mathbf{P}^{-1}\mathbf{A}\mathbf{P} = [\Lambda]. \tag{11}$$

Here **P** represents the modal matrix and $[\Lambda]$ represents a diagonal matrix that has the eigenvalues of **A** on its diagonal.

## SOLUTION OF LINEAR EQUATIONS OF MOTION

The linear equations of motion (Equation (9)) can now be solved by introducing a set of normal or modal coordinates that are related to the state variables through the modal matrix as follows:

$$y_i = \sum_m P_{im} z_m \quad (i,m = 1,...,2N) \tag{12}$$

where the $P_{im}$ are the elements of the modal matrix **P**. Substituting this relationship into the linear equations with external inputs and premultiplying that equation by $P_{ri}^{-1}$ leads to a set of uncoupled differential equations for the modal coordinates that may be written as follows:

$$\dot{z}_r = \lambda_r z_r + f_r \quad (r = 1,...,2N) \tag{13}$$

where

$$f_r = \sum_k \bar{B}_{rk} v_k = \sum_{i,k} P_{ri}^{-1} B_{ik} v_k. \tag{14}$$

Equation (13) represents a set of uncoupled complex-valued first-order ordinary differential equations for the $z_r$. As shown in Reference 12, the general solution to Equation (13) can be found by using the integrating factor $e^{-\lambda_r t}$; the solution may then be written in either of the two equivalent forms

$$z_r = H_r e^{\lambda_r t} + e^{\lambda_r t} \int e^{-\lambda_r \tau} f_r(\tau) d\tau \quad (r = 1,...,2N) \tag{15}$$

or

$$z_r = z_r(0) e^{\lambda_r t} + e^{\lambda_r t} \int_0^t e^{-\lambda_r \tau} f_r(\tau) d\tau \quad (r = 1,...,2N). \tag{16}$$

5

Here the $H_r$ $(r = 1,...,2N)$ represent $2N$ arbitrary constants of integration and the $z_r(0)$ $(r = 1,...,2N)$ are the values of the $z_r$ at time $t = 0$. The values of the state variables can now be recovered by substituting the right sides of either Equation (15) or (16) into Equation (12) to give

$$y_i = \sum_r P_{ir}\left\{ H_r e^{\lambda_r t} + e^{\lambda_r t} \int e^{-\lambda_r \tau} f_r(\tau) d\tau \right\} \qquad (17)$$

or

$$y_i = \sum_r P_{ir}\left\{ z_r(0) e^{\lambda_r t} + e^{\lambda_r t} \int_0^t e^{-\lambda_r \tau} f_r(\tau) d\tau \right\}. \qquad (18)$$

Equations (17) or (18) give the general solution to the linear dynamical equations of motion of the $N$ degree of freedom finite-segment model of a towed system with arbitrary external excitation.

## ANALYSIS OF SYSTEM MOTIONS BY MODE SUPERPOSITION

Motions of a towed system that can be described by the linear equations represented in Equation (9) can be written as linear combinations of the eigenvectors of that system. First, z (0), the initial modal vector is determined from y (0) the initial state vector as follows:

$$z(0) = P^{-1}y(0). \qquad (19)$$

The entries of the modal vector can then be substituted into Equation (18) to determine the system's motion throughout time.

Note that because the motions represented by the $y_i$ on the left sides of Equation (18) are real-valued, the sum on the right side must also be real. As discussed in Reference 12, this requires that underdamped modes be excited in complex conjugate pairs. Corresponding to each such pair of modes is a pair of modal coordinates that are themselves complex conjugates of each other. So then, if only $p_i$ and $p_j$, a single pair of underdamped (complex conjugate) modes are excited, the resulting time-varying state vector can be written as follows:

$$y(t) = z_i(t)p_i + z_j(t)p_j = z_i p_i + \bar{z}_i \bar{p}_i = z_i p_i + \overline{(z_i p_i)} \qquad (20)$$

where $z_i$ and $z_j$ represent the two complex conjugate modal coordinates associated with $p_i$ and $p_j$ and the overbars represent complex conjugates. Because the right side of Equation (20) is the sum of a complex conjugate pair, the resulting state vector is real-valued. In general, therefore, the sum presented by Equation (18) will always be real-valued since complex values always appear in complex-conjugate pairs.

Note also that for systems undergoing external excitation, the above observations indicate an underlying structure for the $\bar{B}$ array defined in Equation (14). In particular, if $z_i$ and $z_j$ represent a pair of complex conjugate modal coordinates, then $\bar{B}_{ik} = \overline{(\bar{B}_{jk})}$ $(k = 1,...,M)$ to ensure proper excitation of both modes.

## REDUCED NONLINEAR EQUATIONS IN MODAL VARIABLES

Using the techniques outlined in the previous section, the reduced nonlinear Equations (6) can also be transformed into modal variables. This is accomplished by substituting from Equation (12) into Equation (6) and premultiplying by $P_{ti}^{-1}$ and simplifying. The result is a set of differential equations for the modal coordinates that may be written as follows:

$$\dot{z}_t = \lambda_t z_t + \sum_k \bar{B}_{tk} v_k + \frac{1}{2} \sum_{r,s} \bar{C}_{trs} z_r z_s + \frac{1}{2} \sum_{k,l} \bar{D}_{tkl} v_k v_l + \sum_{m,k} \bar{E}_{tmk} v_k z_m \quad (t=1,...,2N) \qquad (21)$$

where

$$\bar{B}_{tk} = \sum_i P_{ti}^{-1} B_{ik} \qquad \bar{C}_{trs} = \sum_{i,j,m} P_{ti}^{-1} C_{ijm} P_{jr} P_{ms} \qquad (22)$$

$$\bar{D}_{tkl} = \sum_i P_{ti}^{-1} D_{ikl} \qquad \bar{E}_{tmk} = \sum_{i,j} P_{ti}^{-1} E_{ijk} P_{jm}. \qquad (23)$$

Equation (21) represents a set of complex-valued first-order ordinary differential equations for the $z_t$ that are coupled through the quadratic nonlinearities. Unlike the linear uncoupled equations represented by Equation (13), these equations are not so easily solved. To better understand the structure of these equations, some comments on the properties of the $\bar{C}, \bar{D}$, and $\bar{E}$ arrays may be helpful at this point. As with the $C$ and $D$ arrays of Equation (6), the $\bar{C}$ and $\bar{D}$ arrays possess the following symmetry properties:

$$\bar{C}_{trs} = \bar{C}_{tsr} \ (t,r,s = 1,...,2N) \qquad \bar{D}_{tkl} = \bar{D}_{tlk} \ (t = 1,...,2N; k,l = 1,...,M). \qquad (24)$$

Also, as a result of the fact that the modal variables associated with pairs of complex conjugate modes must themselves be complex conjugates of each other, additional symmetries must exist for the $\bar{B}, \bar{C}, \bar{D}$, and $\bar{E}$ arrays. In particular, if $p_i$ and $p_j$ represent a pair of complex conjugate modes, then the following relationships hold:

$$\bar{C}_{iii} = \overline{(\bar{C}_{jjj})} \qquad \bar{C}_{iij} = \overline{(\bar{C}_{jji})} \qquad \bar{C}_{ijj} = \overline{(\bar{C}_{jii})} \qquad (25)$$

$$\bar{B}_{ik} = \overline{(\bar{B}_{jk})} \qquad \bar{D}_{ikl} = \overline{(\bar{D}_{jkl})} \qquad (k,l = 1,...,M) \qquad (26)$$

$$\bar{E}_{iik} = \overline{(\bar{E}_{jjk})} \qquad \bar{E}_{ijk} = \overline{(\bar{E}_{jik})} \qquad (k = 1,...,M). \qquad (27)$$

To fully understand the effects of quadratic nonlinearities on the modal response of underwater towed systems, Equations (21) must be solved as $2N$ coupled equations. As with the fully nonlinear Equations (1) and (2), this can be done by numerical integration; unfortunately, anlaytical solutions

to these equations are generally not available. This approach provides perfectly acceptable solutions; however, to gain significant insight into the fundamental dynamical behavior of these systems, many such numerical solutions must be generated and studied. This trial-and-error process is very tedious.

Actually, a close examination of Equations (21) for sample systems shows that these equations are not fully coupled. Consider, for example, the towed system of Figure 2, consisting of a sphere and a 100-foot cable being towed at 5 knots with no side currents. The modes for this system may be separated into two basic categories: 1) modes that describe motions in the vertical plane of the mean-ship motion (referred to here as in-plane modes; and 2) modes that describe motions of the system out of this plane (referred to here as out-of-plane modes). Inspection of the numerically generated $\tilde{C}$ matrix for this case shows that the coefficients coupling some of the in-plane and out-of-plane modes are small, indicating the possibility that coupling between those modes can be ignored.

Unfortunately, even taking advantage of these simplifications still leaves one with too many equations for analytical methods. However, if these equations are further simplified by ignoring most or all of the mode coupling, perturbation (asymptotic) expansions may be sought to provide approximate analytical solutions. To this end, the following section describes how the method of multiple scales may be applied to the equation for a single underdamped mode and notes some of the insights gained.

## NONLINEAR PERTURBATION ANALYSIS

As mentioned above, the nonlinear dynamic response of towed systems can be modeled by nonlinear equations of the form of Equations (1) and (2). If we neglect cubic and higher nonlinearities, Equations (1) and (2) can be reduced to the form shown in Equations (6), and these equations can, in turn, be transformed into a set of equations for modal (or normal) variables as shown in Equation (21). Even though these equations are not fully coupled, application of analytical perturbation techniques to solve these equations is impractical. Hence, to apply procedures such as the method of multiple scales to find approximate solutions to the equations, further simplifications must be made. Obviously, simplifications made without sound justification may lead to erroneous conclusions; consequently, any conclusions drawn from such analyses must be verified by returning to the numerical solution of the fully nonlinear Equations (1) and (2).

As a first step, it will be assumed that all modes (except for complex-conjugate pairs) are decoupled, allowing a single equation to be written for each mode. The following sections outline the form of the equation for an underdamped mode with tow point excitation and the application of the method of multiple scales to develop an asymptotic solution to the equation.

## EQUATION FOR AN UNDERDAMPED MODE

Ignoring the coupling between separate modes and noting the symmetries that exist in the $\bar{B}$, $\tilde{C}$, $\bar{D}$, and $\tilde{E}$ arrays given in equations (25) through (27) for modal variables corresponding to

complex conjugate modes, the equation for a single underdamped mode of a towed system excited by tow point motion perturbations can be shown to be of the following form:

$$\frac{dz_r}{d\tau} = \delta_r z_r + \alpha_r z_r^2 + \beta_r \bar{z}_r^2 + \gamma_r z_r \bar{z}_r + \hat{\phi}_r(\tau)z_r + \hat{\psi}_r(\tau)\bar{z}_r + \hat{\eta}_r(\tau) \tag{28}$$

where

$$\tau \ (nondimensional \ time) = |\lambda_r| t \qquad \delta_r = \lambda_r/|\lambda_r| \tag{29}$$

$$\alpha_r = (\bar{C}_{rrr})/2|\lambda_r| \qquad \beta_r = (\bar{C}_{r\bar{r}\bar{r}})/2|\lambda_r| \qquad \gamma_r = (\bar{C}_{r\bar{r}} + \bar{C}_{r\bar{r}r})/2|\lambda_r| = (\bar{C}_{r\bar{r}})/|\lambda_r| \tag{30}$$

where the indices "$r$" and "$s$" represent the complex conjugate mode numbers, and overbars represent complex conjugates. For harmonic tow point excitation, the forcing terms $\hat{\phi}_r(\tau)$, $\hat{\psi}_r(\tau)$, and $\hat{\eta}_r(\tau)$ may be written in the following form:

$$\hat{\phi}_r(\tau) = \hat{Q}_{r1}e^{i\omega\tau} + \hat{Q}_{r2}e^{-i\omega\tau} \qquad \hat{\psi}_r(\tau) = \hat{Q}_{s1}e^{i\omega\tau} + \hat{Q}_{s2}e^{-i\omega\tau} \tag{31}$$

$$\hat{\eta}_r(\tau) = \hat{R}_{r1}e^{i\omega\tau} + \hat{R}_{r2}e^{-i\omega\tau} + \hat{R}_{r3}(2 + e^{i2\omega\tau} + e^{-i2\omega\tau}) \tag{32}$$

where the nondimensional frequency $\omega$ is related to the forcing frequency $\hat{\omega}$ as follows: $\omega = \hat{\omega}/|\lambda_r|$. The values of the $\hat{Q}_{ri}$ and the $\hat{Q}_{si}$ in the above equations are functionally dependent on the excitation amplitude and frequency and elements of the $\bar{E}$ array; the $\hat{R}_{ri}$ are functionally dependent on the excitation amplitude and frequency and elements of the $\bar{B}$ and $\bar{D}$ arrays. Consequently, the $\hat{Q}_{ri}$, the $\hat{Q}_{si}$, and the $\hat{R}_{ri}(i = 1, 2)$ are coefficients of terms linear in the external input perturbations, and the $\hat{R}_{r3}$ are coefficients of terms that are quadratic in the external input perturbations.

## MULTIPLE SCALES ANALYSIS

To determine an an approximate solution to Equation (28), the method of multiple scales[13][14] is employed. To this end, a solution is sought for small but finite amplitudes of the form

$$z_r = \varepsilon z_{r1} + \varepsilon^2 z_{r2} + \varepsilon^3 z_{r3} + O(\varepsilon^4) \tag{33}$$

with the time scales $T_i = \varepsilon^i \tau (i = 0, 1, 2)$. To maintain the terms of $\hat{\eta}_r(\tau)$ that are linear in the external input perturbations as first-order effects in this expansion and all other terms as second-order effects, it will be assumed that the forcing terms $\hat{\phi}_r(\tau)$, $\hat{\psi}_r(\tau)$, and $\hat{\eta}_r(\tau)$ may be written in the following form:

$$\hat{\phi}_r(\tau) = \varepsilon(Q_{r1}e^{i\omega\tau} + Q_{r2}e^{-i\omega\tau}) = \varepsilon\phi_r(\tau) \qquad \hat{\psi}_r(\tau) = \varepsilon(Q_{s1}e^{i\omega\tau} + Q_{s2}e^{-i\omega\tau}) = \varepsilon\psi_r(\tau) \tag{34}$$

$$\hat{\eta}_r(\tau) = \varepsilon(R_{rl}e^{i\omega\tau} + R_{r2}e^{-i\omega\tau}) + \varepsilon^2 R_{r3}(2 + e^{i2\omega\tau} + e^{-i2\omega\tau}) = \varepsilon\eta_{rl}(\tau) + \varepsilon^2\eta_{r2}(\tau). \tag{35}$$

Substituting from Equations (33) through (35) into the differential Equation (28) and separating equations based on like powers of $\varepsilon$ gives the following three partial differential equations for the $z_{ri}(i = 1, 2, 3)$:

$$\frac{\partial z_{rl}}{\partial T_0} - \delta_r z_{rl} = \eta_{rl}(T_0) \tag{36}$$

$$\frac{\partial z_{r2}}{\partial T_0} - \delta_r z_{r2} = -\frac{\partial z_{rl}}{\partial T_1} + \alpha_r z_{rl}^2 + \beta_r \bar{z}_{rl}^2 + \gamma_r z_{rl}\bar{z}_{rl} + \phi_r(T_0)z_{rl} + \psi_r(T_0)\bar{z}_{rl} + \eta_{r2}(T_0) \tag{37}$$

$$\frac{\partial z_{r3}}{\partial T_0} - \delta_r z_{r3} = -\frac{\partial z_{r2}}{\partial T_1} - \frac{\partial z_{rl}}{\partial T_2} + 2\alpha_r z_{rl}z_{r2} + \beta_r \bar{z}_{rl}\bar{z}_{r2} + \gamma_r(z_{rl}\bar{z}_{r2} + \bar{z}_{rl}z_{r2}) +$$

$$\phi_r(T_0)z_{r2} + \psi_r(T_0)\bar{z}_{r2}. \tag{38}$$

Using Equation (16), the solution to Equation (36) can be written as follows:

$$z_{rl} = Ae^{\delta_r T_0} + Be^{i\omega T_0} + Ce^{-i\omega T_0} \tag{39}$$

where

$$A = A(T_1, T_2) \qquad B = \frac{-R_{rl}}{\delta_r - i\omega} \qquad C = \frac{-R_{r2}}{\delta_r + i\omega}. \tag{40}$$

As usual with the method of multiple scales, the coefficient $A$ of the homogeneous solution is assumed to be a function of the slower time scales. The dependence of $A$ on these scales will be determined at subsequent levels of the perturbation expansion through the elimination of secular terms.

Substituting now from Equation (39) into the right side of Equation (37) and using the second term on the right side of Equation (16) yields the following equation for the particular solution to Equation (37):

$$(z_{r2})_p = -\frac{\partial A}{\partial T_1}T_0 e^{\delta_r T_0} + \left(\frac{D_1}{\delta_r}\right)e^{2\delta_r T_0} + \left(\frac{D_2}{2\overline{\delta}_r - \delta_r}\right)e^{2\overline{\delta}_r T_0} + \left(\frac{D_3}{\delta_r}\right)e^{(\delta_r + \overline{\delta}_r)T_0} +$$

$$\left(\frac{D_4}{i\omega}\right)e^{(\delta_r + i\omega)T_0} + \left(\frac{-D_5}{i\omega}\right)e^{(\delta_r - i\omega)T_0} + \left(\frac{D_6}{\overline{\delta}_r - \delta_r + i\omega}\right)e^{(\overline{\delta}_r + i\omega)T_0} + \left(\frac{D_7}{\overline{\delta}_r - \delta_r - i\omega}\right)e^{(\overline{\delta}_r - i\omega)T_0} +$$

$$\left(\frac{-D_8}{\delta_r - i2\omega}\right)e^{i2\omega T_0} + \left(\frac{-D_9}{\delta_r + i2\omega}\right)e^{-i2\omega T_0} + \left(\frac{-D_{10}}{\delta_r}\right) + D_{11}e^{\delta_r T_0} \tag{41}$$

where the coefficients $D_1$ through $D_{11}$ may be written as follows:

$$D_1 = \alpha_r A^2 \qquad D_2 = \beta_r \overline{A}^2 \qquad D_3 = \gamma_r A\overline{A} \tag{42}$$

$$D_4 = 2\alpha_r AB + \gamma_r A\overline{C} + AQ_{r1} \qquad D_5 = 2\alpha_r AC + \gamma_r A\overline{B} + AQ_{r2} \tag{43}$$

$$D_6 = 2\beta_r \overline{AC} + \gamma_r \overline{A}B + \overline{A}Q_{s1} \qquad D_7 = 2\beta_r \overline{AB} + \gamma_r \overline{A}C + \overline{A}Q_{s2} \tag{44}$$

$$D_8 = \alpha_r B^2 + \beta_r \overline{C}^2 + \gamma_r B\overline{C} + BQ_{r1} + \overline{C}Q_{s1} + R_{r3} \tag{45}$$

$$D_9 = \alpha_r C^2 + \beta_r \overline{B}^2 + \gamma_r \overline{B}C + CQ_{r2} + \overline{B}Q_{s2} + R_{r3} \tag{46}$$

$$D_{10} = 2\alpha_r BC + 2\beta_r \overline{BC} + \gamma_r(B\overline{B} + C\overline{C}) + CQ_{r1} + BQ_{r2} + \overline{B}Q_{s1} + \overline{C}Q_{s2} + 2R_{r3} \tag{47}$$

$$D_{11} = \frac{-D_1}{\delta_r} + \frac{-D_2}{2\overline{\delta}_r - \delta_r} + \frac{-D_3}{\delta_r} + \frac{-D_4}{i\omega} + \frac{D_5}{i\omega} + \frac{-D_6}{\overline{\delta}_r - \delta_r + i\omega} + \frac{-D_7}{\overline{\delta}_r - \delta_r - i\omega} +$$

$$\frac{D_8}{\delta_r - i2\omega} + \frac{D_9}{\delta_r + i2\omega} + \frac{D_{10}}{\delta_r}. \tag{48}$$

Eliminating the secular term from this equation requires that $(\partial A/\partial T_1) = 0$ and consequently that $A = A(T_2)$. It should also be noted here, however, that this solution is singular whenever any of the denominators in Equation (41) become zero; this occurs when $\omega = 2\Im(\delta_r)$ which makes $\overline{\delta}_r - \delta_r + i\omega = 0$. This condition corresponds to the condition that $\hat{\omega} = 2\Im(\lambda_r)$, that is that the forcing frequency is twice the frequency of free-modal response. An expansion valid in the neighborhood of this singularity is derived in the following section.

To determine how $A$ depends on $T_2$ and to ensure an asymptotic expansion valid through $O(\varepsilon^2)$, one needs only eliminate the secular terms from the right side of Equation (38). Substituting from Equation (39) and Equation (41) into Equation (38) and setting the sum of the secular terms to zero gives the following equation for the coefficient $A$:

$$\frac{\partial A}{\partial T_2} = aA \tag{49}$$

where

$$a = 2\alpha_r\left(\frac{-D_{10}}{\delta_r} - \frac{BE_5}{i\omega} + \frac{CE_4}{i\omega}\right) + 2\beta_r\left(\frac{\overline{B}E_7}{\delta_r - \overline{\delta}_r + i\omega} + \frac{\overline{C}E_6}{\delta_r - \overline{\delta}_r - i\omega}\right) + \gamma_r\left(\frac{-\overline{D}_{10}}{\overline{\delta}_r} + \frac{B\overline{E}_6}{\delta_r - \overline{\delta}_r - i\omega}\right) +$$

$$\gamma_r\left(\frac{C\overline{E}_7}{\delta_r - \overline{\delta}_r + i\omega} + \frac{\overline{B}E_4}{i\omega} - \frac{\overline{C}E_5}{i\omega}\right) + \frac{-Q_{r1}E_5}{i\omega} + \frac{Q_{r2}E_4}{i\omega} + \frac{Q_{s1}\overline{E}_6}{\delta_r - \overline{\delta}_r - i\omega} + \frac{Q_{s2}\overline{E}_7}{\delta_r - \overline{\delta}_r + i\omega} \tag{50}$$

and

$$E_4 = 2\alpha_r B + \gamma_r\overline{C} + Q_{r1} \qquad E_5 = 2\alpha_r C + \gamma_r\overline{B} + Q_{r2} \tag{51}$$

$$E_6 = 2\beta_r\overline{C} + \gamma_r B + Q_{s1} \qquad E_7 = 2\beta_r\overline{B} + \gamma_r C + Q_{s2}. \tag{52}$$

Therefore, an asymptotic expansion for $z_r$ can be written as follows:

$$z_r = \left(\varepsilon\hat{A}e^{a\varepsilon^2 T_0} + \varepsilon^2 D_{11}\right)e^{\delta_r T_0} + \varepsilon Be^{i\omega T_0} + \varepsilon Ce^{-i\omega T_0} + \varepsilon^2\left(\frac{-D_{10}}{\delta_r}\right) +$$

$$\varepsilon^2\left(\frac{D_1}{\delta_r}e^{2\delta_r T_0} + \frac{D_2}{2\overline{\delta}_r - \delta_r}e^{2\overline{\delta}_r T_0} + \frac{D_3}{\overline{\delta}_r}e^{(\delta_r + \overline{\delta}_r)T_0} + \frac{D_4}{i\omega}e^{(\delta_r + i\omega)T_0} + \frac{-D_5}{i\omega}e^{(\delta_r - i\omega)T_0}\right) +$$

$$\varepsilon^2\left(\frac{D_6}{\overline{\delta}_r - \delta_r + i\omega}e^{(\overline{\delta}_r + i\omega)T_0} + \frac{D_7}{\overline{\delta}_r - \delta_r - i\omega}e^{(\overline{\delta}_r - i\omega)T_0} + \frac{-D_8}{\delta_r - i2\omega}e^{i2\omega T_0} + \frac{-D_9}{\delta_r + i2\omega}e^{-i2\omega T_0}\right). \tag{53}$$

As with the particular solution shown in Equation (41), this solution is singular when $\omega = 2\Im(\delta_r)$.

For values of $\omega$ not in the neighborhood of $2\Im(\delta_r)$, Equation (50) can be used to determine numerical values for $a$, and hence, whether the perturbation expansion is bounded or unbounded. For example, should the real part of $a$ be positive for some range of excitation amplitudes and frequencies, it indicates that the free-oscillation terms are large. There are two possible explanations for this occurrance. The first is that the expansion has simply not been carried out to a high enough

12

order to provide a uniform expansion. The second is that the solution for $z_{rl}$ in Equation (39) is fundamentally different in character from the exact solution to Equation (28), indicating that the solution itself may exhibit relatively strong nonlinear characteristics.

Finally, note that Equation (53) contains the constant term $-D_{10}\epsilon^2/\delta_r$ that is indicative of a nonsymmetric cable response about its steady-state configuration. This behavior was noted in References 1 and 5; it is a direct result of the quadratic nature of the fluid drag forces on the system. The fluid forces on the system increase faster as the system moves in the direction of the tow than they decrease as it moves opposite to the direction of the tow. $D_{10}$ has been found to be nonzero for in-plane modes and zero for out-of-plane modes as expected.

## MULTIPLE SCALES ANALYSIS - EXPANSION NEAR SINGULARITY

As mentioned above, the expansion shown in Equation (53) is not valid in the neighborhood of $\omega = 2\Im(\delta_r)$. To develop an expansion that is valid, introduce a so-called detuning parameter $\sigma$ defined such that $\omega = i(\bar{\delta}_r - \delta_r) + \epsilon\sigma = 2\Im(\delta_r) + \epsilon\sigma$. Using this definition converts the term on the right side of Equation (37) responsible for the singularity into a secular term. In particular,

$$D_6 e^{(\bar{\delta}_r + i\omega)T_0} = E_6 \bar{A} e^{i\sigma T_1} e^{\delta_r T_0}. \tag{54}$$

Then, elimination of secular terms leads to the equation:

$$\frac{\partial A}{\partial T_1} - \left(E_6 e^{i\sigma T_1}\right)\bar{A} = 0. \tag{55}$$

Assuming that the secular terms have been omitted, an asymptotic expansion for $z_r$ through $O(\epsilon^2)$ becomes

$$z_r = (\epsilon A(T_1, T_2) + \epsilon^2 D_{11})e^{\delta_r T_0} + \epsilon B e^{i\omega T_0} + \epsilon C e^{-i\omega T_0} + \epsilon^2\left(\frac{-D_{10}}{\delta_r}\right) +$$

$$\epsilon^2\left(\frac{D_1}{\delta_r}e^{2\delta_r T_0} + \frac{D_2}{2\bar{\delta}_r - \delta_r}e^{2\bar{\delta}_r T_0} + \frac{D_3}{\bar{\delta}_r}e^{(\delta_r + \bar{\delta}_r)T_0} + \frac{D_4}{i\omega}e^{(\delta_r + i\omega)T_0} + \frac{-D_5}{i\omega}e^{(\delta_r - i\omega)T_0}\right) +$$

$$\epsilon^2\left(\frac{D_7}{\bar{\delta}_r - \delta_r - i\omega}e^{(\bar{\delta}_r - i\omega)T_0} + \frac{-D_8}{\delta_r - i2\omega}e^{i2\omega T_0} + \frac{-D_9}{\delta_r + i2\omega}e^{-i2\omega T_0}\right). \tag{56}$$

The dependence of $A$ on the time scales $T_1$ and $T_2$ is determined by the elimination of all secular terms. As before, the elimination of secular terms from the right side of Equation (38) leads to the

equation

$$\frac{\partial A}{\partial T_2} = aA \tag{57}$$

where $a$ is now defined to be

$$a = 2\alpha_r\left(\frac{-D_{10}}{\delta_r} - \frac{BE_5}{i\omega} + \frac{CE_4}{i\omega}\right) + + \gamma_r\left(\frac{-\overline{D}_{10}}{\overline{\delta}_r} + \frac{C\overline{E}_7}{\delta_r - \overline{\delta}_r + i\omega} + \frac{\overline{B}E_4}{i\omega} - \frac{\overline{C}E_5}{i\omega}\right) +$$

$$2\beta_r\left(\frac{\overline{B}\overline{E}_7}{\delta_r - \overline{\delta}_r + i\omega}\right) - \frac{Q_{r1}E_5}{i\omega} + \frac{Q_{r2}E_4}{i\omega} + \frac{Q_{r2}\overline{E}_7}{\delta_r - \overline{\delta}_r + i\omega}. \tag{58}$$

Together Equations (55) and (57) can be shown to be equivalent to the differential equation

$$\frac{dA}{d\tau} - (\varepsilon E_6 e^{i\sigma\varepsilon\tau})\overline{A} - (\varepsilon^2 a)A = 0. \tag{59}$$

This equation is a first-order equation with time-varying coefficients; to transform it to an equation with constant coefficients, let $A = Ge^{i\sigma\varepsilon\tau/2}$. Making this substitution, separating into real and imaginary parts, and solving the coupled first-order equations, give the following result:

$$\Re(G) = g_1 e^{\mu_1\tau} + g_2 e^{\mu_2\tau} \tag{60}$$

$$\Im(G) = \left(\frac{\mu_1 - \varepsilon^2\Re(a) - \varepsilon\Re(E_6)}{\frac{\sigma\varepsilon}{2} - \varepsilon^2\Im(a) + \varepsilon\Im(E_6)}\right)g_1 e^{\mu_1\tau} + \left(\frac{\mu_2 - \varepsilon^2\Re(a) - \varepsilon\Re(E_6)}{\frac{\sigma\varepsilon}{2} - \varepsilon^2\Im(a) + \varepsilon\Im(E_6)}\right)g_2 e^{\mu_2\tau} \tag{61}$$

where

$$\mu_{1,2} = \varepsilon^2\Re(a) \pm \varepsilon\sqrt{\rho} \quad \text{if} \quad \rho = |E_6|^2 - \sigma^2/4 + (\varepsilon\sigma + \varepsilon^2)\Im(a) \geq 0$$

$$\mu_{1,2} = \varepsilon^2\Re(a) \pm \varepsilon i\sqrt{-\rho} \quad \text{if} \quad \rho < 0.$$

The first free oscillation term in this expansion grows without bound as $\tau \to \infty$ whenever the amplitude $A$ is unbounded. This occurs when $\rho > 0$ and $\varepsilon\Re(a) \pm \sqrt{\rho} > 0$ and when $\rho < 0$ and $\Re(a) > 0$. As before, this may indicate either that the perturbation solution has not been carried out to a high enough order to provide a uniform expansion or that the solution for $z_{r1}$ in Equation (39) is fundamentally different in character from the exact solution to Equation (28).

## NUMERICAL EXAMPLES

As stated in the previous section, one possible indication of relatively strong nonlinear response of individual modes of the towed system is the presence of unbounded free oscillation terms in the perturbation expansions derived therin. In this section, numerical results are presented for the individual response of two modes of a towed sphere subject to tow point excitations. Results are presented first for an in-plane mode of the system and then for an out-of-plane mode of the system. In particular, values of the arguments of the exponential function that appear in the definition of the coefficient $A$ of the free-response term are presented over the frequency range from $0.01 \rightarrow 5.0$ radians/second. This range is within the response range of many surface ships and includes the free response frequency of the selected modes.

The towed system consists of a 15-inch diameter sphere towed at 15 knots at the end of 150 feet of a 0.54-inch diameter smooth jacketed cable. The sphere weighs 500 pounds in air; the cable weighs 0.39 pounds/foot in air and has a buoyancy of 0.089 pounds/foot in sea water. For modeling purposes, the cable was divided into 10 links (finite-segments) with the longest link at the towed end of the cable and the shortest link at the sphere; this is consistent with the mode shapes of the cable.

The lowest-frequency underdamped mode of this system is an out-of-plane mode and the next lowest-frequency underdamped mode is an in-plane mode. The eigenvalues $\lambda_r$ associated with these modes are

$$\text{Out-of-Plane Mode:} \quad \lambda_r = (-0.69357;\ 1.2480)$$

$$\text{In-Plane Mode:} \quad \lambda_r = (-1.0540;\ 1.4405).$$

The corresponding mode shapes are animated in Figure 3 for one complete cycle of free response assuming no amplitude decay. For the out-of-plane mode, the motion is distributed over the entire length of cable; larger amplitudes are experienced at the free end. In the case of the in-plane mode, most of the motion occurs at the free end of the cable; little motion occurs near the tow point.

For this system, the reduced nonlinear Equations (6) were generated, transformed into the form of Equation (21), and then reduced to a single equation of the form of Equation (28) for each mode and excitation type. The external excitation was applied both *in* and *normal to* the towing plane, the former being referred to as *in-plane excitation* and the latter *out-of-plane excitation*. The in-plane excitation was further subdivided into excitations along and normal to the cable. The non-zero coefficients in Equation (28) for each mode and excitation are summarized in the following table.

15

| | NON-ZERO COEFFICIENTS | |
|---|---|---|
| MODE | In-Plane Excitation | Out-of-Plane Excitation |
| In-Plane | $\alpha_r, \beta_r, \gamma_r, \hat{\phi}_r$ $\hat{\psi}_r, \hat{\eta}_{r1}, \hat{\eta}_{r2}$ | $\alpha_r, \beta_r, \gamma_r, \hat{\eta}_{r2}$ |
| Out-of-Plane | $\hat{\phi}_r, \hat{\psi}_r$ | $\hat{\eta}_{r1}$ |

Note that in the case of out-of-plane excitation of the out-of-plane mode, no quadratic nonlinearities are present; hence, the resulting equation is linear. For in-plane excitation of this mode, quadratic nonlinearities arise only through the forcing terms. The equations for the in-plane mode are more complex. For in-plane excitation of the in-plane mode, all possible quadratic nonlinearities are present. For out-of-plane excitation of this mode, the linear forcing terms and some of the nonlinear forcing terms are absent.

Consider first results for excitation of the in-plane mode. Figure 4 shows the real part and Figure 5 shows the imaginary part of the exponent $a$ of the expansion in Equation (53) for excitation parallel to the towed end of the cable; the excitation amplitude is 0.5 feet (1 foot peak to trough) and is applied over the frequency range $0.01 \leq \hat{\omega} \leq 5.0$ radians/second. Note that results for the range $2.8 \leq \hat{\omega} \leq 3.0$ radians/second have been omitted to avoid the singularity at $\hat{\omega} = 2\Im(\lambda_r) = 2.881$ radians/second. Even though the real part of $a$ appears unaffected by the presence of the singularity, it is clear from Figure 5 that the imaginary part of $a$ is affected by the presence of the singularity. In fact, if one plots the real and imaginary parts of $a$ over the range $2.8 \leq \hat{\omega} \leq 3.0$ radians/second, it is clear that both values are affected.

For an expansion in the neighborhood of this frequency, an expansion of the form of Equation (56) is sought; the coefficient $A$ must satisfy Equation (59). Unfortunately, as shown in Figure 6, the real part of $\mu_1$ is positive (albeit small) over this range. However, as the excitation amplitude is lowered, the frequency range over which the exponents have positive real parts becomes smaller and smaller around the singularity. In conclusion, the perturbation expansions developed above are bounded throughout the frequency range shown, except in the neighborhood of $\hat{\omega} = 2\Im(\lambda_r) = 2.881$ radians/second. Bounded solutions can be found closer and closer to this frequency by lowering the excitation amplitude.

Next, consider excitation of the in-plane mode perpendicular to the towed end of the cable. Figure 7 shows the real part, and Figure 8 shows the imaginary part of the exponent $a$ of the expansion in Equation (53) for an excitation amplitude of 0.5 feet (1 foot peak to trough) over the frequency range $0.01 \le \hat{\omega} \le 5.0$ radians/secons. Note that, as above, results for the range $2.8 \le \omega \le 3.0$ radians/secons have been omitted to avoid the singularity when $\hat{\omega} = 2\Im(\lambda_r) = 2.881$ radians/second. Unlike the above case, the real part of $a$ is positive over the entire range of frequencies shown. Moreover, lowering the excitation amplitude to 0.001 feet simply lowers the values of the exponents, but they remain positive. Hence, even for extremely small excitation, the perturbation expansion is unbounded. This is true in the neighborhood of the singularity as well.

The results for out-of-plane excitation of this mode are shown in Figure 9. The real part of $a$ is negative over the entire frequency range, indicating a bounded expansion. Note that, unlike the case of in-plane excitation, no singularity exists in this case because the coefficient $D_6$ in Equation (41) is zero, hence eliminating the singular term in the expansion.

Consider finally, results for excitation of the out-of-plane mode. Since Equation (28) reduces to a linear equation for out-of-plane excitation of the out-of-plane mode, perturbation methods are not required to study its response when cubic and higher order nonlinearities are ignored. For in-plane excitation of this mode, the steady-state solution is zero and nonzero response exists only for nonzero initial conditions; that is, the modal coordinate simply relaxes from its perturbed initial state back to zero. For in-plane excitation along or normal to the cable, the real part of $a$ is zero for all frequencies, and the imaginary part of $a$ is near zero except very near the singularity at $\hat{\omega} = 2\Im(\lambda_r)$. Hence, the perturbation expansion is bounded at all frequencies, except at frequencies very near the singularity. A plot of the imaginary part of $a$ for in-plane excitation normal to the cable is shown in Figure 10. As in the cases above, using detuning around the singularity still resulted in an unbounded expansion. Also, as before, as the amplitude of the external excitation is lowered, bounded expansions can be found closer to the the singularity point.

As a cross-check of the above results, the differential equations governing the modal variables were numerically integrated at selected excitation frequencies. The results of the integration of the equations (of the form of Equation (28)) containing the quadratic nonlinearities were compared with those of the integration of the linearized forms of these equations. These comparisons led to the following conclusions. First, in cases where $\Re(a)$ is negative, the differences between the linear and nonlinear solutions were relatively small in comparison to the cases when $\Re(a)$ is positive. Also, as $\Re(a)$ gets larger (more positive), the nonlinear behavior becomes stronger. In general, the results suggest that $\Re(a)$ can be used to indicate how nonlinear the response of individual modes are to harmonic excitation. This is consistent with the notion that perturbation methods may be applied most successfully to weakly nonlinear systems.

It should be noted here that numerical integration uncovered no particularly unusual behavior at the singular point $\hat{\omega} = 2\Im(\lambda_r)$. As a result, this singularity should not be considered an indication of highly nonlinear behavior but rather a product of the perturbation expansion itself.

17

# SUMMARY

This paper presents the methodology for developing perturbation expansions to describe the response of individual modes of a towed system to tow point excitation using the method of multiple scales. The equations of perturbed motion (up through quadratic nonlinearities) are developed about a general steady-state equilibrium configuration using a numerical, finite-segment computer program used at the Coastal Systems Station to model the nonlinear dynamics of towed cable systems.

Results are shown for two modes of a sphere towed at 15 knots from a 150-foot cable; one of the modes is characterized by motions in the towing plane (in-plane) and the other is characterized by motions normal to the towing plane (out-of-plane). Each mode was subjected to in-plane and out-of-plane harmonic excitation at the system's tow point. The results indicate that the out-of-plane mode responds linearly to out-of-plane excitation, but that the in-plane mode has nonlinear response to in-plane excitation. For the towed sphere system presented, the strength of the nonlinear response depends on the direction of the in-plane excitation; excitation normal to the towed end of the cable is shown to produce a stronger nonlinear response than excitation parallel to the cable. Weak nonlinear response is characterized by a bounded perturbation expansion and strong nonlinear response is characterized by an unbounded expansion.

Perturbation expansions for in-plane excitation of in-plane modes are shown to have a singularity when the excitation frequency is twice the free-response frequency of that mode. The frequency range over which the expansion breaks down can be narrowed by lowering the excitation amplitude.

Numerical integration of the differential equations governing the modal variables (associated with the above modes) supports the conclusions drawn from the perturbation analysis. However, no unusual behavior was found at the frequency associated with the singularity in the perturbation expansion, indicating that the singularity was a product of the expansion alone and not an indicator of highly nonlinear behavior.

The present analysis could be easily extended to include systems with external excitations at locations other than the system tow point, such as, say, the control surfaces of a towed vehicle. It can also be extended to study the coupled response of pairs of modes of towed systems and the effects of cubic nonlinearities. The procedure can be used to investigate the fundamental dynamic properties of towed systems and could possibly be used to generate low-order dynamic models that include a minimal number of modes to describe system dynamics. Numerical integration of the equations of motion of such models can be compared with numerical integration of the fully nonlinear Equations (1) and (2) to determine the accuracy of these models.
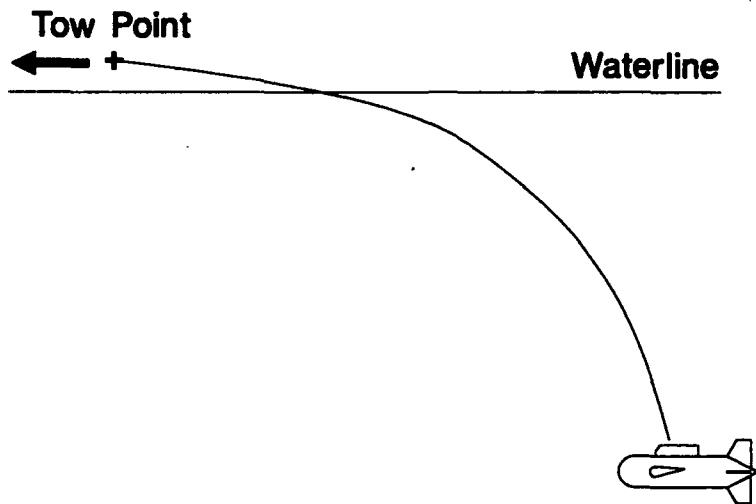
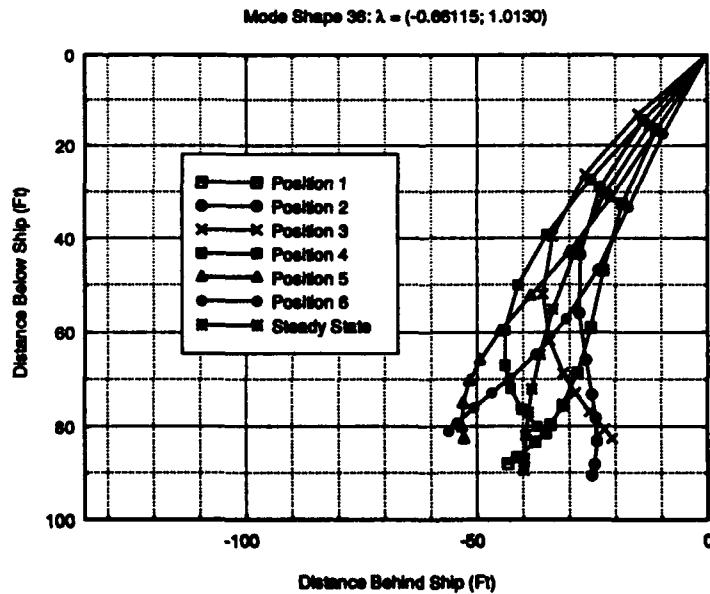**FIGURE 1. TOWED SYSTEM WITH A SINGLE VEHICLE AND TOW CABLE**



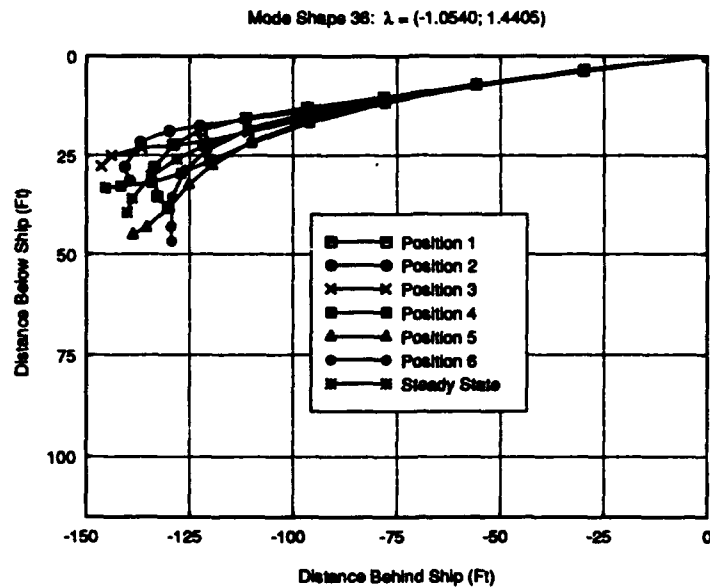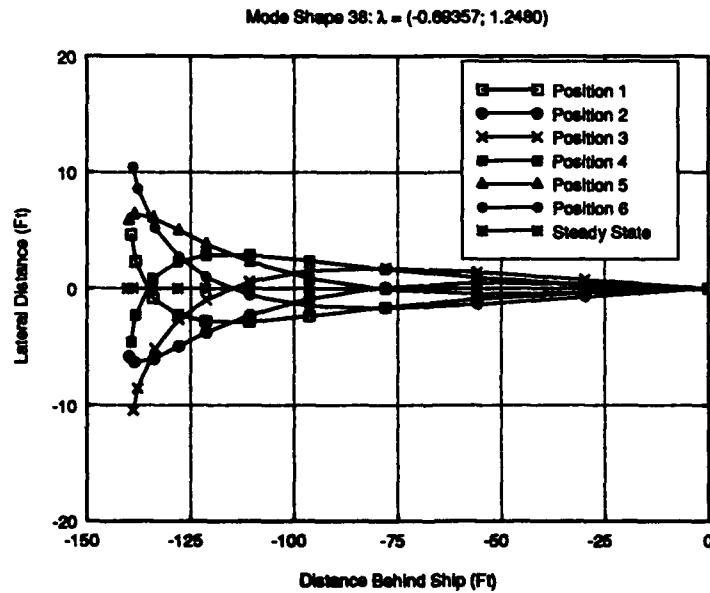**FIGURE 2. MODE SHAPE OF 100 -FOOT CABLE WITH SPHERE AT 5 KNOTS**

Mode Shape 36: λ = (-1.0540; 1.4405)



**a. IN-PLANE MODE**

Mode Shape 36: λ = (-0.68357; 1.2480)



**b. OUT-OF-PLANE MODE**

**FIGURE 3. MODE SHAPE OF 150 -FOOT CABLE WITH SPHERE
AT 15 KNOTS**

Argument of Exponential Function from Perturbation Analysis



**FIGURE 4. REAL PART OF EXPONENT** $a$ **FROM PERTURBATION ANALYSIS: IN-PLANE EXCITATION, ALONG CABLE**

Argument of Exponential Function from Perturbation Analysis
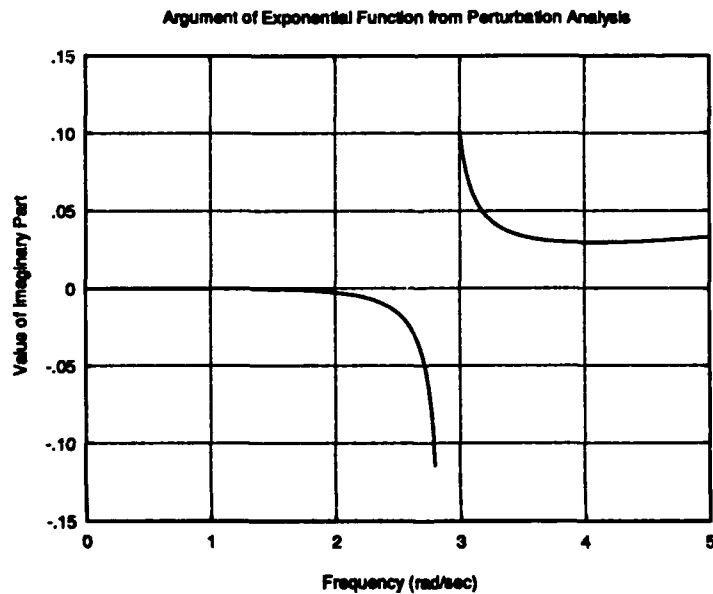


**FIGURE 5. IMAGINARY PART OF EXPONENT** $a$ **FROM PERTURBATION ANALYSIS: IN-PLANE EXCITATION, ALONG CABLE**

Argument of Exponential Function from Perturbation Analysis
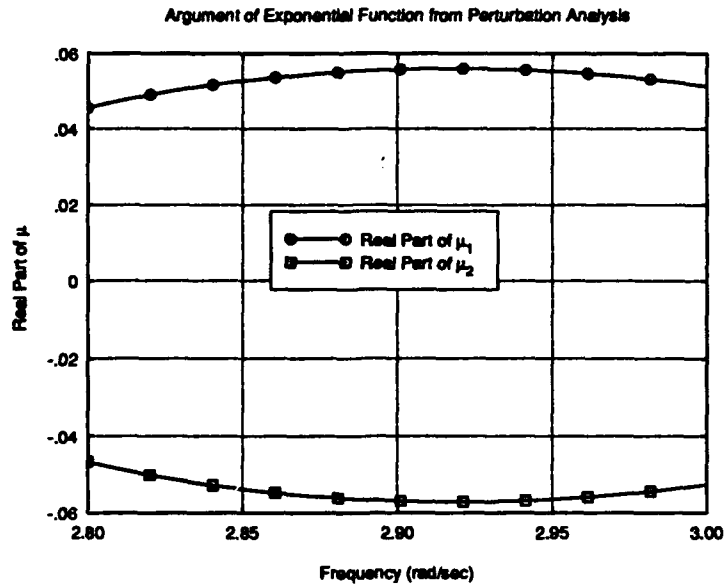


**FIGURE 6. REAL PARTS OF EXPONENTS $\mu_1$ AND $\mu_2$ FROM PERTURBATION ANALYSIS: IN-PLANE EXCITATION, ALONG CABLE**

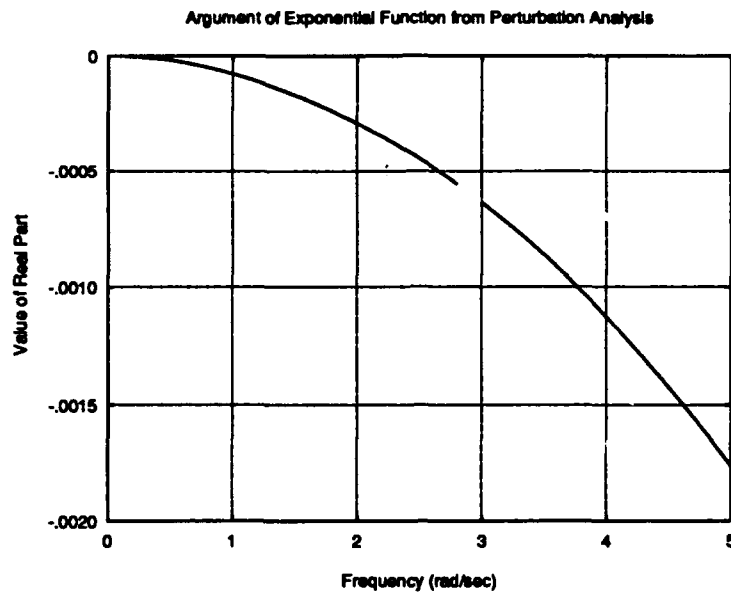Argument of Exponential Function from Perturbation Analysis
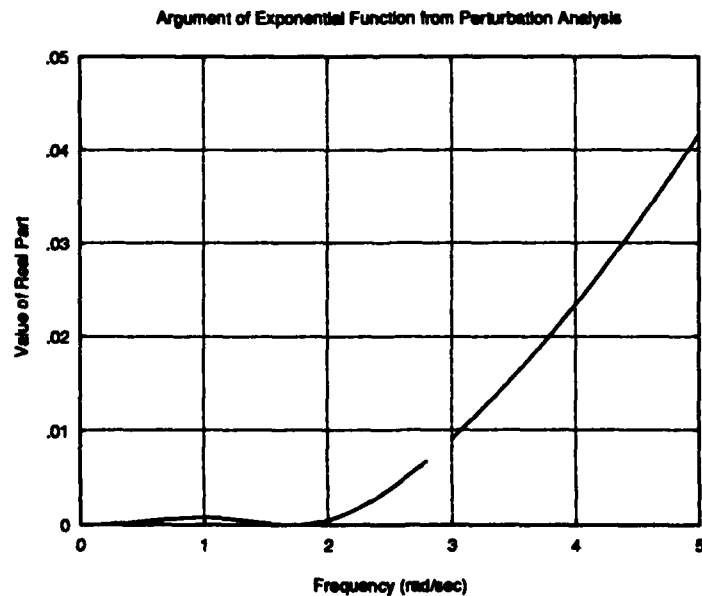


**FIGURE 7. REAL PART OF EXPONENT $a$ FROM PERTURBATION ANALYSIS: IN-PLANE EXCITATION, NORMAL TO CABLE**

**FIGURE 8. IMAGINARY PART OF EXPONENT $a$ FROM PERTURBATION ANALYSIS: IN-PLANE EXCITATION, NORMAL TO CABLE**



**FIGURE 9. EXPONENT $a$ FROM PERTURBATION ANALYSIS: OUT-OF-PLANE EXCITATION**

23

Argument of Exponential Function from Perturbation Analysis

**FIGURE 10. IMAGINARY PART OF EXPONENT $a$ FROM PERTURBATION ANALYSIS: IN-PLANE EXCITATION, NORMAL TO CABLE**

## REFERENCES

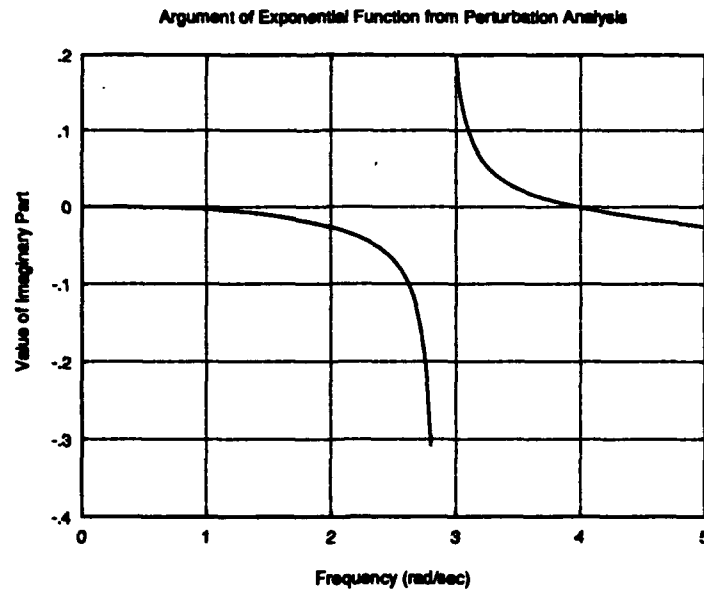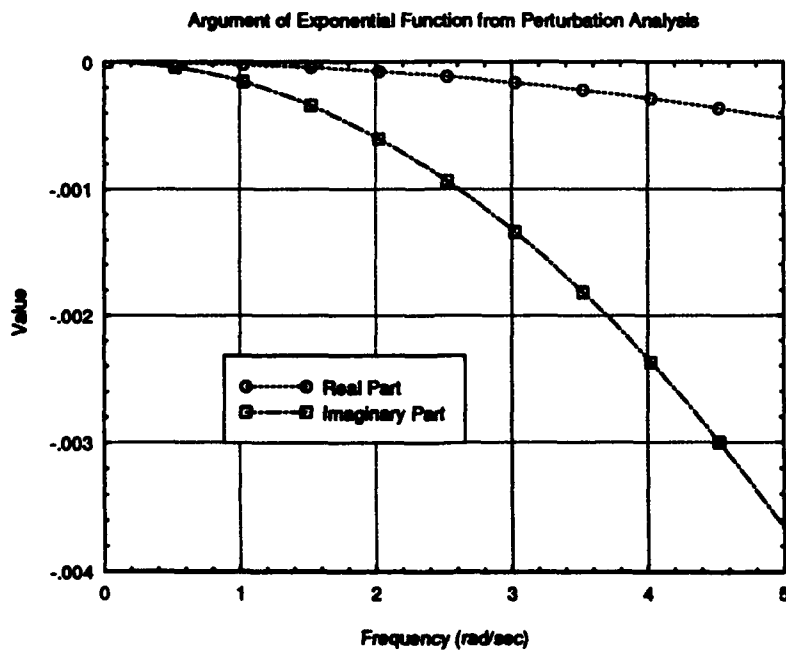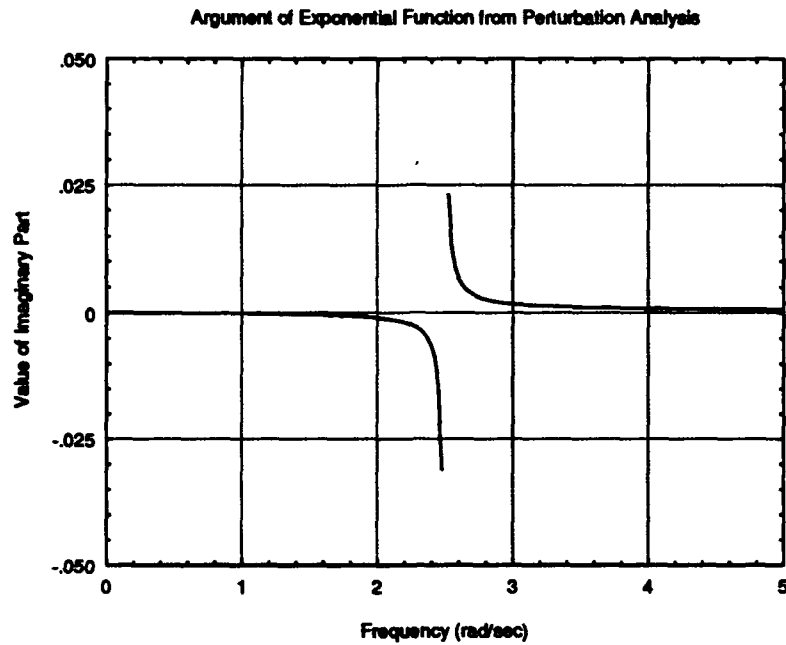1.    D.A. Chapman, "Effects of Ship Motion on a Neutrally-Stable Towed Fish," *Journal of Ocean Engineering*, Vol. 9, No. 3, pp. 189-220, 1982.

2.    H.T. Wang, "Three-Dimensional Long-Time Motion Behavior of Ocean Cable Systems," Proceedings of the Second International Offshore Mechanics and Arctic Engineering Symposium, January, 1983.

3.    C.M. Ablow and S. Schechter, "Numerical Simulation of Undersea Cable Dynamics," *Journal of Ocean Engineering*, Vol. 10, No. 6, pp. 443-457,1983.

4.    J.W. Kamman and R.L. Huston, "Modelling of Submerged Cable Dynamics," *Computers and Structures*, Vol. 20, No. 1-3, pp. 623-629, 1985.

5.    J.W. Kamman and T.C. Nguyen, "Modeling Towed Cable System Dynamics," NCSC TM 492-88, Naval Coastal Systems Center, Panama City, FL, 1988.

6.    P.J. Wingham and B. Ireland, "The Dynamic Behavior of Towed Airborne and Underwater Body-Cable Systems," Advances in Underwater Technology, Ocean and Offshore Engineering, Vol. 15: Technology Common to Aero and Marine Engineering, Society for Underwater Technology, 1988.

7.    D.W. Baker, C.K. Holberger, and D. Janas, "Computer Simulation of Towed System Dynamics," Proceedings of the OCEANS 89 Conference, pp. 1498-1503, Seattle, WA, September, 1989.

8.    T.N. Delmer and T.C. Stephens, "Numerical Simulation of an Oscillating Towed Weight," *Journal of Ocean Engineering*, Vol. 16, No. 2, pp. 143-172, 1989.

9.    J.W. Kamman, T.C. Nguyen, and J.W. Crane, "Modeling Towed Cable System Dynamics," Proceedings of the OCEANS 89 Conference, pp. 1484-1489, Seattle, WA, September, 1989.

10.   M.S. Triantafyllou and F. Hover, "Cable Dynamics for Tethered Underwater Vehicles," Massachusetts Institute of Technology Sea Grant Program Report No. MITSG90-4, Cambridge, MA, 1990.

11.   R.B. Chiou and J.W. Leonard, "Nonlinear Hydrodynamic Response of Curved Singly-Connected Cables," Proceedings of the Second Conference on Computer Modeling in Ocean Engineering, Barcelona, Spain, October, 1991.

12.   D.E. Newland, "On the Modal Analysis of Non-Conservative Linear Systems," *Journal of Sound and Vibration*, Vol. 112, No. 1, pp. 69-96, 1987.

13.   A.H. Nayfeh, *Introduction to Perturbation Techniques*, John Wiley & Sons, Inc., New York, 1981.

14.   A.H. Nayfeh and D.T. Mook, *Nonlinear Oscillations*, John Wiley & Sons, Inc., New York, 1979.

15.   K.A. Foss, "Co-Ordinates Which Uncouple the Equations of Motion of Damped Linear Systems," *Journal of Applied Mechanics*, Vol. 25, pp. 361-364, 1958.

## DISTRIBUTION LIST

Copy No.

Office of Naval Research
800 North Quincy Street
Arlington, VA 22217-5000
(Code 1121, Dr. S. Ramberg)                                    1


Commander
Naval Sea Systems Command
Naval Sea Systems Command Headquarters
Washington, DC 20362-5101
(Library)                                                      2
(PMS 407B, D. Grembi)                                          3


Chief of Naval Operations
Navy Department
Washington, DC 20350-2000                                      4


Commander
David Taylor Research Center
Bethesda, MD 20084-5000
(Library )                                                     5
(Code 1541, R. Knutson)                                        6
(Code 1541, Dr. P. Rispin)                                     7


Commanding Officer
Naval Underwater Systems Center
Newport, RI 02840
(Library)                                                      8
(Code 3342, N. Topolsky)                                       9


Commanding Officer
Naval Oceans Systems Center
San Diego, CA 92132
(Library)                                                     10


Commanding Officer
Naval Research Laboratory
Washington, DC 20375
(Library)                                                     11
(Dr. H. Whang)                                                12

Commander
Naval Surface Weapons Center
White Oak
Silver Spring, MD 20910
(Library)                                                                   13


Commander
Naval Surface Weapons Center
Dahlgren Laboratory
Dahlgren, VA 22448
(Library)                                                                   14


Superintendent
US Naval Academy
Annapolis, MD 21402-5000
(Library)                                                                   15


Superintendent
US Naval Postgraduate School
Monterey, CA 93943
(Library)                                                                   16


Chief of Naval Research
800 North Quincy Street
Arlington, VA 22217-5000
(Code 20)                                                                   17
(Code 235, W. Ching)                                                        18


Commander
Naval Air Systems Command
Naval Air Systems Command Headquarters
Washington, DC 20361-5101
(Library)                                                                   19
(PMA 210C, H. Scheetz)                                                      20


Commanding Officer
Naval Civil Engineering Laboratory
Port Hueneme, CA 93043
(Library)                                                                   21
(Code L40PM, D. Shields)                                                    22

Commander
Mine Warfare Command
Naval Base
Charleston, SC 29408-5500
(Library)                                                    23
(Code N4A, G. Pollitt)                                       24


Administrator
Defense Technical Information Center
Cameron Station
Alexandria, VA 22304-6145                                    25-26